High Energy Astrophysics

First Test Data from the CANGAROO Project for Stereo Čerenkov Imaging

P.G. Edwards, A.G. Gregory, J.R. Patterson, M.D. Roberts, G.P. Rowell, N.I. Smith, G.J. Thornton, N.R. Wild, *Department of Physics and Mathematical Physics, University of Adelaide, Adelaide SA 5000*

H. Fujii, S. Kabe, Y. Watase, *National Laboratory for High Energy Physics, Tsukuba 305, Japan*

M. Fujimoto, *National Astronomical Observatory, Tokyo 181, Japan*

T. Hara, *Yuge Mercantile Marine College, Yuge 794–25, Japan*

N. Hayashida, T. Kifune, M. Teshima, *Institute for Cosmic Ray Research, University of Tokyo, Tokyo 188, Japan*

F. Kakimoto, S. Ogio, T. Tanimori, T. Yoshikoshi, *Department of Physics, Tokyo Institute of Technology, Tokyo 152, Japan*

Y. Mizumoto, T. Suda, *Department of Physics, Kobe University, Kobe 657, Japan*

Y. Matsubara, Y. Muraki, Solar Terrestrial Environment Laboratory, Nagoya University, Nagoya 464–01, Japan

Abstract: The CANGAROO project incorporates two Čerenkov imaging telescopes at Woomera to obtain stereo images of very high-energy gamma-ray (and cosmic-ray) showers. The first stereo observations, with one imaging system, were made in March 1992, and preliminary stereo imaging observations began in July 1992. This paper describes the stereo imaging technique, the sources under investigation, and the indications from the first data sets.

1. Introduction

Very high-energy gamma-ray astronomy is ground-based. The flux of gamma rays at these energies, E > 100GeV, is too low for detection by the present generation of satellite experiments. The atmospheric Čerenkov technique allows the indirect detection of these gamma rays. The technique is limited to clear, moonless nights—at most about 10% of the year—but suffers a more severe complication from the overwhelming background of cosmic-ray initiated showers. Significant progress in the field has been made only relatively recently, with the adoption of techniques to reject a large majority of the cosmic ray background. The Čerenkov imaging technique has been shown to be a very powerful technique in this regard, and will be described in more detail below. Reviews of the field can be found elsewhere (Weekes 1992, Clay and Dawson 1992).

The Earth's atmosphere plays a key role in very high-energy (VHE) gamma-ray astronomy. Incident gamma rays and cosmic rays interact with atmospheric nuclei and through the processes of pair production and bremsstrahlung produce an extensive air shower, or cascade. Electrons and positrons in the cascade with energies greater than ~21 MeV and muons with energies greater than ~4.3 GeV produce Čerenkov radiation in a narrow cone about their direction of travel. The cone half-angle varies with refractive index (as do the threshold energies for Čerenkov emission), and hence with altitude, but is ~1° over the relevant height range.

The cascade develops laterally about the shower core (which corresponds to the direction of the incident gamma ray or cosmic ray). In gamma-ray showers this is due principally to Compton scattering of the electrons and positrons. In cosmic-ray showers, the pions produced in the hadronic interactions of the primary cosmic ray and its secondary particles are created with appreciable transverse momenta, which are subsequently inherited by their decay products. At very high energies the particle cascade is relatively quickly absorbed by the atmosphere—with the exception of the muon component of cosmic-ray showers the cascade particles do not reach sea-level. However the predominantly blue Čerenkov light produced by the relativistic particles in the cascade undergoes only moderate atmospheric loss.

As a result of the emission angle and the lateral spread of the cascade, the Čerenkov light pool at sea-level has a radius of typically 150 m for a shower from the zenith. Simulations reveal that the lateral distribution of Čerenkov photons within this radius is very flat, and falls off steeply outside it (e.g., Hillas and Patterson 1990). Hence, unlike other forms of astronomy, where the collecting area is defined by the physical dimensions of the telescope, in VHE gamma-ray astronomy the collecting area is defined by the Čerenkov light pool. A modest telescope therefore has a large collecting area, typically $3 \times 10^4 m^2$, facilitating the detection of gamma-ray showers at an appreciable rate despite the intrinsically low flux, typically less than $10^{-6} m{-}2 s^{-1}$.

2. The Čerenkov Imaging Technique

The realisation that the structure of shower images could be utilised to differentiate between gamma-ray and cosmic-ray showers arose from detailed simulations of the Čerenkov images. Moment-fitting procedures allow the images, which to a first approximation can be regarded as ellipses, to be characterised by their width, length and orientation. In physical terms, the length of an image is a measure of the longitudinal development of the cascade, whereas the width is closely related to the lateral structure of the cascade.

Two distinct factors distinguish the images from gamma rays (from a point source being tracked by the telescope) from the isotropic cosmic-ray background: differences in the size and/or shape of the image, and differences in orientation of the image. Gamma rays images tend to be more compact, and with their major axis pointing towards the centre of the field of view. The hadronic nature and penetrating muon component of cosmic-ray showers result in these producing more ragged and diffuse images. Furthermore, because cosmic rays arrive randomly from all directions, their images are randomly oriented (Hillas and Patterson 1990).

The imaging technique was pioneered by the Whipple group and resulted in the highly significant detection, and

subsequent confirmation, of unpulsed TeV gamma rays from the Crab Nebula (Weekes *et al.* 1989, Vacanti *et al.* 1991). More recently the Whipple group has detected TeV gamma rays from the active galaxy Markarian 421 (Punch *et al.* 1992), following its earlier detection by the EGRET detector on board the Compton Gamma Ray Observatory. The Whipple group has shown that a careful selection of image parameter cuts allows more than 97% of cosmic-ray showers to be rejected, with the loss of only ~50% of gamma-ray showers (Weekes 1992).

3. The Bicentennial Gamma Ray Telescope

As described in Edwards *et al.* (1992), the University of Adelaide has operated a VHE gamma-ray telescope near Woomera since 1988. Briefly, the Bicentennial Gamma-Ray Telescope (BIGRAT) consists of three 4.1m diameter composite mirrors on a common alt-azimuth mount. As it is relevant to the discussion later, we briefly review the original detector configuration. A detector "pod" of three 51 mm diameter photomultipliers was located in the focal plane of each of the three mirrors (see Figure 1a). A triple coincidence within ~8 ns of the discriminated outputs of any set of three photomultipliers in corresponding positions in the three detector pods (i.e., viewing the same region of sky) formed the event trigger. This condition ensures a negligible chance coincidence rate, despite individual photomultipler rates (above the discriminator level) of up to 50kHz. Specifically, the three mirrors are denoted A, B and C, and the three tubes in a triplet denoted 1, 2 and 3. An event may therefore have arisen from triggering only one set of three corresponding photomultipliers, e.g., A1, B1 and C1, (hereafter a single), or from simultaneously triggering two sets (a double), or from triggering all nine photomultipliers.

In July 1992 an imaging camera was installed in the focal plane of the central mirror. Prior to this, the central mirror was upgraded with the installation of off-axis paraboloids. The point spread function for the central mirror is now ~15′ fwhm, about the size of the camera pixels. The camera consists of thirty-seven 13mm x 13mm square photomultipliers, and has a 2.5° aperture. The camera is surrounded by a ring of eight 51mm diameter photomultipliers centred 2.2° from the axis, which are used to monitor off-source regions of sky. Flexibility has been added to the outer pods, which may operate with their previous triplets of 51mm photomultipliers, or with a single 76mm photomultiplier on axis (see Figure 1b). A triple coincidence of corresponding photomultipliers from the outer pods with 'overlapping' camera pixels forms the event trigger. From October 1992, the signal from each photomultiplier will be passed to an analog-to-digital converter (ADC), and recorded for each event. Until then, 'hit-patterns' will be recorded for all events, i.e., those photomultipliers with signals above the discrimination level will be flagged, but no information on the signal size is available. ADC information enables a full imaging analysis to be made, and allows an estimate of the energy of the primary gamma ray or cosmic ray to be obtained. The present camera event rate near vertical is ~4.5 Hz for the triplet and ~3 Hz for the 76mm single tubes corresponding to energy thresholds of ~500 GeV and ~600 GeV respectively.

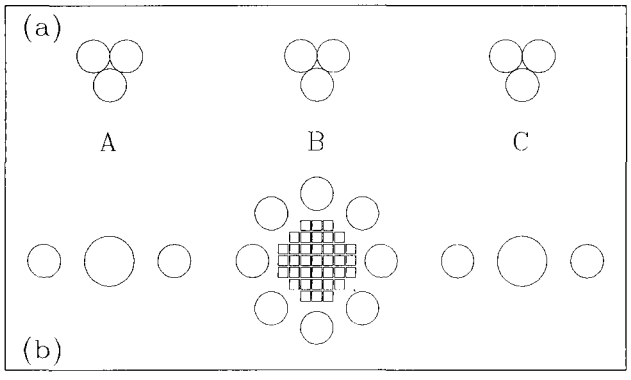

Figure 1: Two different layouts of photomultipliers in BIGRAT detector pods. The three composite mirror/detector pod systems are labelled A, B and C. Figure 1a shows the original triplet detectors of three 51mm photomultipliers in each pod. The three photomultipliers in the A pod are named A1, A2 and A3, and corresponding photomultipliers in B named B1, B2 and B3 etc. Figure 1b shows one of the possible set-ups utilising the imaging camera. The camera is located in the focal plane of the central mirror, and is surrounded by eight 51mm photomultipliers. The outer pods contain either a single 75mm photomultiplier as illustrated, or alternatively an original triplet, between two "monitor" 51mm photomultipliers. The Japanese 3.8m telescope is located 100m to the east of BIGRAT, and contains an imaging camera of 220 pixels.

A second, independent technique for cosmic-ray shower rejection is also being developed. The output pulses from a 76mm-photomultiplier, in the focal plane of one of the outer mirrors, are digitised by a Tektronix 7912 transient digitiser. The system has a bandwidth of ~180 MHz, imposed mainly by the signal cable bandwidth. Monte carlo simulations suggest that the Cerenkov light pulses associated with gamma-ray showers are narrower and smoother than those of cosmic ray showers. By excluding events with pulses resembling those expected for cosmic-ray showers, the signal-to-noise ratio of the data should be enhanced. The simulations indicate that a rise-time cut is probably the most effective method of separating the two.

4. The Japanese 3.8m-telescope

The Japanese side of the collaboration operate a 3.8m diameter telescope, which was transported from Mt Dodaira to Woomera at the beginning of 1991. (Mt Dodaira is shown in the discussion of light pollution by Isobe and Sugihara (1991)). The 3.8m diameter, composite mirror, telescope was previously used for lunar ranging, and has a significantly better angular resolution than the current generation of purpose-built TeV telescopes. The telescope has been fitted with an imaging camera of two hundred 10mm x 10mm square photomultipliers, giving a field of view of ~2.7°.

The summed output of all photomultipliers is used to determine the event trigger, with an additional requirement that the signal in at least 4 photomultipliers must exceed the 2~3 photo-electron level. The large number of photomultipliers coupled with a necessarily wider ADC input gate-width result in a significant number of camera pixels being triggered by sky noise, starlight, etc. Many such triggers can be discarded due to their low signal level, and extra discrimination is obtained with the use of time-to-digital converters to record the arrival time of the signal in each photomultiplier. Signals associated with a shower image are generally bunched within several nanoseconds, and signals outside this grouping can be discarded. The 4-fold trigger is biased slightly towards detecting gamma-ray showers, as they are more concentrated than cosmic-ray showers. The observed event rate of ~1 Hz at zenith corresponds to an energy threshold of about 1 TeV.

5. CANGAROO

The ability of the imaging technique to select preferentially gamma-ray initiated showers is further improved by operating in coincidence with a second telescope ~100 m away. This arises as, for those showers detected by both telescopes, the orientation of the shower image in two different planes can usually be found. Studies with data from the single Whipple telescope have shown that a stereo system can locate very high-energy gamma-ray sources with arc minute accuracy (Akerlof *et al.* 1991). This is the motivation for the CANGAROO project.

The CANGAROO (Collaboration between Australia and Nippon for a Gamma-Ray Observatory in the Outback) project utilises the two imaging telescopes described above to make stereo observations of potential TeV gamma-ray sources. The Japanese telescope is situated 100 m to the east of BIGRAT. The 100m spacing is a compromise between maximising the angular resolution (which improves with separation) and the stereo event rate (which decreases with separation). An east-west baseline was chosen to optimise the projected baseline for northern and southern celestial objects. The two telescopes are operated independently, though they will usually track the same source. Cables connecting the two systems allow stereo events to be flagged in real-time.

A rubidium clock has been used since the beginning of the University of Adelaide's work at Woomera to determine the arrival time of recorded events. The Japanese data taking system accesses the arrival time from the same clock to ensure compatibility of the data. The long term stability of the clock is monitored by regular checks at the GPS/Tranet tracking station at the Defence Science and Technology Organisation, Salisbury.

6. Sources and Observations

A variety of celestial objects are potential emitters of TeV gamma rays. These include X-ray binaries (e.g., Gregory *et al.* 1990), pulsars and associated supernova remnants (e.g., Weekes *et al.* 1989), and extragalactic objects (e.g., Punch *et al.* 1992). Only relatively nearby galaxies are expected to be detectable at TeV energies as the TeV gamma-ray flux is absorbed by the infrared background (Stecker *et al.* 1992).

The imaging technique is most effective at small zenith angles. As noted in Weekes *et al.* (1989), the size of shower images decreases with increasing zenith angle. The decrease is mainly in image width. Energy threshold increases with zenith angle, and higher energy showers penetrate further into the atmosphere, resulting in a slower decrease in image length with zenith angle. In their observation of the Crab, Weekes *et al.* only observed at zenith angles less than 55°, with the majority of their observations made at angles less than 30°.

This decrease in image size is evident in pre-camera BIGRAT data. Figure 2 plots the ratio of double events to single (see section 3) events as a function of zenith angle. (Recall, the overwhelming majority of these events are cosmic-ray events.) As the zenith angle increases, proportionally fewer events are doubles. This is particularly evident beyond ~50°, and is consistent with shower images becoming narrower, and therefore less likely to overlap two sets of photomultipliers. The data at ~70° are from observations of northern celestial hemisphere objects, such as Cygnus X-3 and Hercules X-1, made using the low elevation technique (Sommers and Elbert 1987).

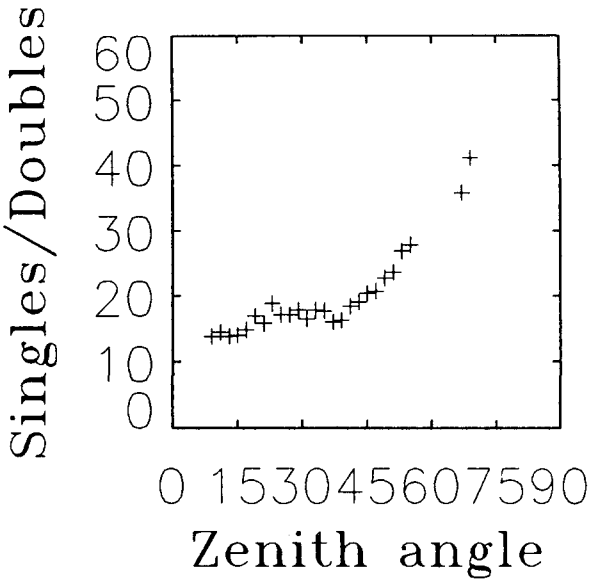

Figure 2: Compilation of BIGRAT data obtained with the original triplet detectors. The ratio of singles (events triggering one set of three photomultipliers) to doubles (events triggering two sets of three) is plotted as a function of zenith angle. The increase in the ratio with zenith angle is consistent with a decrease in image size. Simulations reveal the decrease occurs mainly in the width of the image.

The first 'hit pattern' imaging data from BIGRAT confirms the decrease of image size with increasing zenith angle. Events triggering the camera at large zenith angles trigger, on average, 3.1 camera pixels and 0.2 monitor photomultipliers per event, compared to an average of 6.3 pixels and 1.0 monitor photomultipliers per event at the zenith. (Data taken by simulating triggers with a signal generator indicate that roughly one pixel per three events is triggered by night sky background photons.)

As a result, candidate sources to be observed with the imaging technique will be mainly those observable at moderate zenith angles. The Crab Nebula—the standard candle at TeV energies—transits at 52° when viewed from Woomera. Although not an ideal zenith angle, observations will be made using both the imaging and pulse-shape techniques.

Figure 3 displays two BIGRAT hit patterns. Figure 3a is a typical cosmic-ray event image; it is relatively large, and not oriented towards the centre of the field of view. In contrast, Figure 3b is a candidate gamma-ray event, narrower and oriented towards the centre of the camera. The installation of ADCs in the BIGRAT camera electronics in October 1992 will allow information on image parameters to be extracted from images.

Some single-telescope observing will continue, but we anticipate most observations will use the stereo imaging technique. Figure 4 results from one of the first stereo observations, made in March 1992 tracking Centaurus A. At the time the 3.8m telescope had a 180 pixel imaging camera operating, whilst BIGRAT was using its three 51mm triplet detectors. During the 1.5 hr stereo observation, the 3.8m event rate averaged 0.4 Hz, as opposed to the 4 Hz rate of BIGRAT. The rate of stereo events was thus determined by the 3.8m rate. Of the ~2130 events recorded by the 3.8m, ~27% were able to be analysed for their image parameters, i.e., width, length, image centroid, etc. (This low figure reflects the preliminary nature of this early observation, and results in part from noise contamination suffered by the 3.8m electronics at the time, but since remedied.) Of the

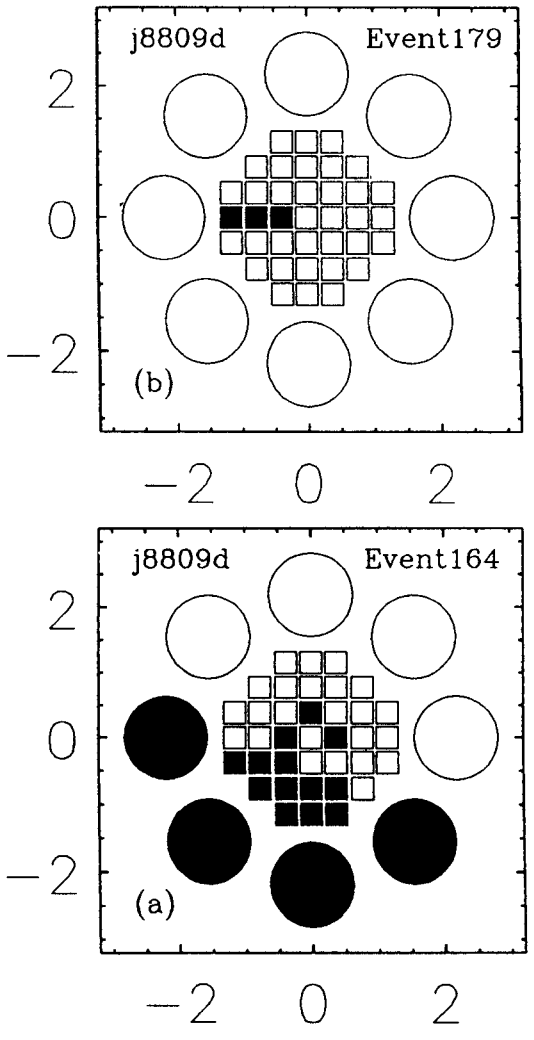

Figure 3: Examples of hit patterns obtained with BIGRAT imaging camera. The squares represent 10mm x 10mm photomultipliers of the camera, and the circles represent the 51mm diameter "monitor" photomultipliers surrounding the camera. Figure 2a is an example of a cosmic ray event, where shaded elements correspond to those photomultipliers above the discrimination level. Figure 2b is an example of the kind of image expected for gamma ray initiated showers—narrower, and pointing towards the centre of the field of view (when the telescope is tracking the source). The axes are labelled with focal plane angular coordinates in degrees.

~575 events assigned image parameters, ~50% were stereo events, i.e., events detected by both telescopes. The overall number of stereo events was roughly double this, but not all stereo events meet the 3.8m imaging analysis requirements.

As a check on the quality of the imaging, Figure 4 displays, for BIGRAT single events only, the 3.8m focal plane image centroid for the three classes of single events; the 1s (i.e., those triggering A1, B1 and C1), 2s and 3s. The distance of the image centroid from the centre of the field of view is related to the physical distance from the telescope to the shower core. The passage of the shower core through the atmosphere, the major axis of the image and the image centroid all lie in the same plane. Figure 4 reveals that events triggering A1, B1 and C1 fall preferentially in one third of the 3.8m field of view, and similarly for 2s and 3s triggers. This is as expected: stereo events will usually fall between the two telescopes, and it is not surprising that those showers with cores falling in e.g., the A1-B1-C1 field of view should generally fall in a region of similar size in the 3.8m 289focal plane. (Both telescopes are alt-azimuth mounts,

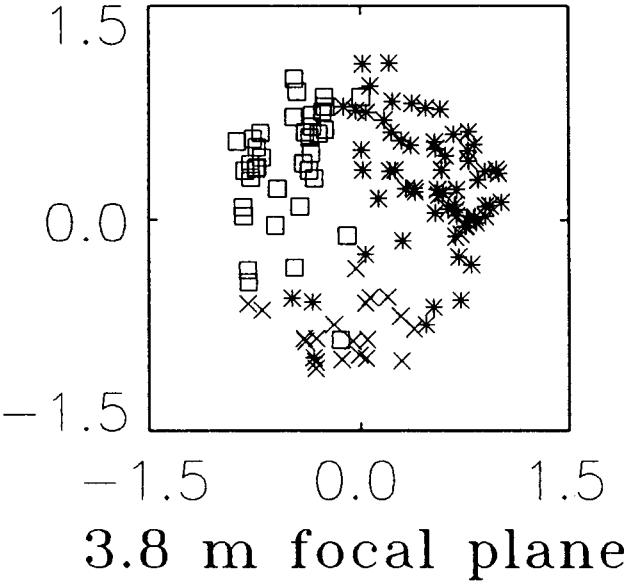

Figure 4: The distribution of image centroids in the 3.8m focal plane for stereo data. At this time BIGRAT was using three sets of 51mm diameter triplet detectors. The squares represent those events triggering one set of three BIGRAT detectors (A1, B1 and C1); the triangles those stereo events triggering BIGRAT detectors A2, B2 and C2, and the plus signs the stereo events triggering A3, B3 and C3. The clustering of these three subsets of stereo events is explained in the text.

and so both fields of view rotate in the same way as a source is tracked.)

These preliminary results are in accord with expectations, and augur well for the commencement of full stereo imaging later this year.

Acknowledgements

This work is supported by Grants-in-Aid for Scientific Research from Monbusho (the Japanese Ministry of Education, Science and Culture), the Australian Research Council, DITAC's International Science and Technology Program and the University of Adelaide. PGE gratefully acknowledges the receipt of a Queen Elizabeth II Fellowship, and thanks Peter Atanackovic, David Baker, Syd Dowden, Tim Dyke, Gary Hill, Andrew Horton, Anthony Lee, Rishi Meyhandan, Janice Reid and Kylie Waring for their assistance.

Akerlof, C.W., Cawley, M.F., Chantell, M., Fegan, D.J., Harris, K., Hillas, A.M., Jennings, D.G., Lamb, R.C., Lawrence, M.A., Lang, M.J., et al., 1991, *Astrophys. J.*, **377**, L97.

Clay, R.W. and Dawson, B.R., 1992, *Proc. Astron. Soc. Aust.*, in press.

Edwards, P.G., Gregory, A.G., Patterson, J.R., Roberts, M.D., Rowell, G.P., Smith, N.I., Wild, N.R., Ebisuzaki, S., Fujii, H., Kabe, S., et al., 1992, *Proc. Astron. Soc. Aust.*, **10**, 27.

Gregory, A.G., Patterson, J.R., Roberts, M.D., Smith, N.I. and Thornton, G.J., 1990, *Astron. Astrophys.*, **237**, L5.

Hillas, A.M. and Patterson, J.R., 1990, J. *Phys. G: Nucl. Phys.*, **16**, 1271.

Isobe, S. and Sugihara, N., 1991, *Proc. Astron. Soc. Aust.*, **9**, 336.

Punch, M., Akerlof, C.W., Cawley, M.F., Chantell, M., Fegan, D.J., Fennell, S., Gaidos, J.A., Hagan, J., Hillas, A.M., Jiang, Y., et al., 1992, *Nature*, **358**, 477.

Sommers, P. and Elbert, J., 1987, *J. Phys. G: Nucl. Phys.*, **13**, 553.

Stecker, F.W., de Jager, O.C. and Salamon, M.H., 1992, *Astrophys. J.*, **390**, L49.

Vacanti, G., Cawley, M.F., Colombo, E., Fegan, D.J., Hillas, A.M., Kwok, P.W., Lang, M.J., Lamb, R.C., Lewis, D.A., Macomb, D.J. et al., 1991, *Astrophys. J.*, **377**, 467.

Weekes, T.C., Cawley, M.F., Fegan, D.J., Gibbs, K.G., Hillas, A.M., Kwok, P.W., Lamb, R.C., Lewis, D.A., Macomb, D., Porter, N.A. et al., 1989, *Astrophys. J.*, **342**, 379.

Weekes, T.C., 1992, *Space. Sci. Rev.*, **59**, 315.